RSC Advances

PAPER

View Article Online
View Journal | View Issue

Cite this: *RSC Adv.*, 2021, **11**, 21991

Preparation, characterization, and feasibility study of Sr/Zn-doped CPP/GNS/UHMWPE composites as an artificial joint component with enhanced hardness, impact strength, tribological and biological performance†

Kaixuan Zhang,[a] Xu Peng,[b] Can Cheng,[a] Yang Zhao[a] and Xixun Yu *[a]

In order to solve the problem of aseptic loosening of artificial joints resulting from the wear particles of artificial joint components in total joint replacement (TJR), we synthesized a new kind of metalo-organic particle (Sr/Zn-doped CPP/GNS) using spark plasma sintering (SPS) as a filler to enhance the comprehensive performance of UHMWPE. Sr/Zn-doped CPP/GNS was interfused evenly with UHMWPE particles and cured in a hot press instrument to prepare Sr/Zn-doped CPP/GNS/UHMWPE composites. FTIR and SEM were carried out to characterize Sr/Zn-doped CPP/GNS particles. EDS was carried out to characterize Sr/Zn-doped CPP/GNS/UHMWPE. The micro-structure, hardness, impact strength, tribology and bio-activities of Sr/Zn-doped CPP/GNS/UHMWPE composite materials were also investigated. The results confirmed the effectiveness of this method. The hardness, impact strength, and tribology of the composites were enhanced by adding homodispersed Sr/Zn-doped CPP/GNS particles into UHMWPE. In the meantime, Sr/Zn-doped CPP/GNS/UHMWPE composites could significantly promote the growth of osteoblasts due to the bio-activity of Sr/Zn-doped CPP/GNS. Furthermore, the addition of Sr/Zn-doped CPP/GNS particle-fillers into UHMWPE could promote the secretion of OPG from osteoblasts and inhibit the secretion of RANKL from osteoblasts, and thus increase the OPG/RANKL ratio. All the results above showed that Sr/Zn-doped CPP/GNS/UHMWPE composites with appropriate Sr/Zn-doped CPP/GNS content possessed superior physicochemical performances and bio-properties, and could be considered as promising materials to treat aseptic loosening in total joint replacement.

Received 26th March 2021
Accepted 19th May 2021

DOI: 10.1039/d1ra02401a

rsc.li/rsc-advances

Introduction

As a useful and widespread treatment for severe arthritis, total joint replacement (TJR) reduces the pain of patients by improving the function of the weight-bearing joint.[1–3] Owing to its outstanding properties (such as chemical inertness and impact resistance), ultra-high molecular weight polyethylene (UHMWPE) is extensively used in orthopedic surgery to construct artificial joint components.[4] However, there is a disadvantage in its application. The wear particles of UHMWPE inhibit the formation of bone and promote bone resorption, which causes failure in the healing of the joint with osteolysis and joint loosening.[4–6] Great pain is caused to patients due to these pathological reactions in surrounding tissues. This pathological phenomenon is referred to as the aseptic loosening of artificial joints.[7] The long-term successful application of artificial joints after TJR is limited by the aseptic loosening of the artificial joint.[3]

Previous studies implied that the wear properties of UHMWPE can be improved by doping with filler. Sobajima *et al.* used multiwall carbon nanotubes (MWCNTs) to enhance UHMWPE, and the results exhibited good properties.[8] Mindivan *et al.* used reduced graphene oxide (RGOC) to enhance UHMWPE by liquid phase ultrasonic mixing and hot press molding, and RGOC/UHMWPE showed excellent tribological behavior as a bio-material.[9] Chen *et al.* used grapheme oxide (GO) to prepare GO/NaCl/UHMWPE by hot pressing and the anti-friction and anti-wear properties of GO/NaCl/UHMWPE were improved with the water-based lubrication.[10] Zhipeng Gu *et al.* used Sr-doped calcium polyphosphate (SCPP) as a filler to prepare SCPP/UHMWPE composites, and the composite with a suitable SCPP content had potential efficacy to prevent and treat aseptic loosening.[11] However, the bioproperty of preventing aseptic loosening of UHMWPE had not been greatly improved after doping with SCPP filler; moreover, its impact strength decreased sharply with the addition of SCPP. Thus, we

[a]*College of Polymer Science and Engineering, Sichuan University, Chengdu 610065, P. R. China. E-mail: yuxixun@163.net*

[b]*Experimental and Research Animal Institute, Sichuan University, Chengdu 610065, P. R. China*

† Electronic supplementary information (ESI) available. See DOI: 10.1039/d1ra02401a

must find a method to improve both the physicochemical performance and bio-properties of UHMWPE.

Our previous studies showed that SCPP had potential pharmaceutical efficacy to prevent and treat aseptic loosening.[12–14] Many studies suggested that zinc incorporation also could enhance bone repair.[15,16] Zinc has the ability to boost the expression of genes, including OPG (osteoprotegerin) and RANKL (receptor activator of nuclear factor-κ B ligand) in the process of co-culturing with osteoblast.[17] We can deduce that Sr and Zn have a synergistic effect in promoting the formation of bone and inhibiting bone resorption after introducing Sr and Zn into CPP (calcium polyphosphate). We can expect that Sr/Zn-doped CPP will have more significant pharmaceutical efficacy to prevent and treat aseptic loosening. In order to strengthen the mechanical properties of Sr/Zn-doped CPP filler and then improve the physicochemical properties of the Sr/Zn-doped CPP/UHMWPE composite, we also combined graphene carbon nanosheets (GNS) with Sr/Zn-doped CPP.

In this paper, Sr/Zn-doped CPP/GNS (the sintering product of Sr/Zn-doped CPP and GNS) was prepared using spark plasma sintering (SPS). As a non-conventional powder consolidation method in processing novel materials, SPS has widened the envelope of processing conditions available to produce biomaterials with novel micro-structure architectures.[18] In this technique, the consolidation of powders was done with a short sintering cycle, which is the result of the pulsing electric field, resistance heating, and high pressure.[19] A solid-state mixing method using ball-milling and flat-panel curing is adopted to prepare Sr/Zn-doped CPP/GNS/UHMWPE composites, which have the potential to be used as joint components. Their hardness, impact strength and tribology were examined. The *in vitro* bio-activities of particles on cells were tested by CCK-8 and ELISA. The results of this research can provide a promising novel material with great comprehensive performance in impact strength, wear-resistance, and biological efficacy for fabricating an acetabular cup (all abbreviations appearing in the main article are listed in ESI Table 1†).

Experimental

Preparation of Sr/Zn-doped CPP/GNS

Zinc–strontium-doped calcium phosphate mono-basic monohydrate was prepared according to the following steps. Zinc carbonate hydroxide (AR, Aladdin), strontium carbonate (AR, Aladdin) and calcium carbonate (AR, Aladdin) were slowly added into phosphoric acid (AR, Aladdin) under stirring at a constant speed. The molar ratio of phosphoric acid to carbonate was about 2.5. After reacting at room temperature for 12 h, the aged solution was evaporated in a vacuum. Then the precipitates were washed with ethanol (AR, Aladdin) until the pH of the filtrate was about 7. The reaction equations are as follows:

$$CaCO_3 + 2H_3PO_4 \rightarrow Ca(H_2PO_4)_2\cdot H_2O + CO_2$$

$$xCaCO_3 + ySrCO_3 + z[3Zn(OH)_2\cdot 2ZnCO_3] + 2H_3PO_4 \rightarrow Ca_xSr_yZn_{5z}(H_2PO_4)_2\cdot H_2O + CO_2$$

The homogeneous amorphous Sr/Zn-doped CPP powder was prepared according to the following steps. The strontium-doped calcium phosphate mono-basic mono-hydrate powders were calcined at 500 °C for 10 h to yield Sr/Zn-doped CPP. Then they were heated to 1100 °C at a rate of 15°C min^{-1}. After holding them at 1100 °C for 1 h, the melt was quenched in distilled water to avoid crystallization. Finally, the amorphous products were milled in a machine to get powders in the size range of 5 μm.

The reaction equations are as follows:

$$Ca_xSr_yZn_{5z}(H_2PO_4)_2\cdot H_2O \rightarrow Ca_xSr_yZn_{5z}(H_2PO_4)_2 + H_2O$$

$$Ca_xSr_yZn_{5z}(H_2PO_4)_2 \rightarrow Ca_xSr_yZn_{5z}H_2P_2O_7 + H_2O$$

$$kCa_xSr_yZn_{5z}H_2P_2O_7 \rightarrow kCa_xSr_yZn_{5z}(PO_3)_2 + kH_2O$$

The Sr/Zn-doped CPP/GNS metalo-organic particles were prepared by spark plasma sintering according to the following steps. The graphene nanosheets (AR, Chengdu Organic Chemical Co., Ltd. Chinese Academy of Sciences) and Sr/Zn-doped CPP powders (self-made) were mixed using a homogenizer at 3000 rpm for 3 min in ethanol to get uniform powders. After drying in a vacuum drying oven, the powders were compacted in the cylindrical graphite mold of the spark plasma sintering instrument (SL LABOX-650F, Japan). The mold was heated to 280 °C at a rate of 140°C min^{-1} with 40 MPa pressure at both ends. After sintering at 280 °C for 8 minutes, the final products were cooled to room temperature and milled. The final product was named Sr/Zn-doped CPP/GNS. The dose of strontium in Sr/Zn-doped CPP/GNS particles was set at 8% (Sr/Ca molar ratio) due to it having the best performance.[11] Meanwhile, the dose of zinc was controlled at 0.1%, 0.15%, 0.2%, 0.25%, or 0.3% (Zn/Ca molar ratio).

Characterization of Sr/Zn-doped CPP/GNS

FTIR, SEM, and XPS were used to characterize the Sr/Zn-doped CPP/GNS. The Sr-doped CPP, Sr/Zn-doped CPP, Sr/Zn-doped CPP + GNS (the solid mixed product of amorphous Sr/Zn-doped CPP powders and graphene sheets), and Sr/Zn-doped CPP/GNS powders were respectively mixed with potassium bromide (KBr) to prepare thin tablets for FTIR spectroscopy analysis. The FTIR spectra of the samples were obtained using an FTIR spectrometer (Bomem MB-120) at a frequency in the range of 400–4000 cm^{-1}. The morphological determination of Sr/Zn-doped CPP/GNS was carried with a Scanning Electron Microscope (JSM-5900LV, JEOL) at a magnification of 4000× and an accelerating voltage of 20 kV. The elemental analysis of Sr/Zn-doped CPP/GNS was performed with X-ray photo-electron spectroscopy (AXIS Supra, KRATOS).

Preparation of Sr/Zn-doped CPP/GNS/UHMWPE

Ultra-high molecular weight polyethylene (UHMWPE) was purchased from Mitsui Chemicals Inc. with an average viscosity molecular weight of 2.5×10^6. We chose six Sr/Zn-doped CPP/GNS contents against UHMWPE at 0%, 5%, 10%, 15%, 20%, and 30% (w/w) to prepare homogeneous solid-state mixtures.

UHMWPE and Sr/Zn-doped previously prepared CPP/GNS were uniformly mixed in ethanol using a homogenizer at 3000 rpm for 10 min to get uniform powders. The mixed powders were dried using a vacuum drying oven. The powders were added into the mold ($80 \times 10 \times 4$ mm^3) and put into the hot press instrument (China). After discharging gas bubbles by preheating for 15 min without pressure at 200 °C, the agglomerates were pressed for 30 min under a pressure of 10 MPa and then cooled to room temperature. Thus the Sr/Zn-doped CPP/GNS/UHMWPE were prepared.

Characterization of Sr/Zn-doped CPP/GNS/UHMWPE

The elemental analysis of Sr/Zn-doped CPP/GNS/UHMWPE was carried out using an Energy Dispersive Spectrometer (AXIS Ultra DLD, KRATOS) under the observation of a Scanning Electron Microscope (JSM-5900LV, JEOL) at 20 kV.

Hardness of Sr/Zn-doped CPP/GNS/UHMWPE

A durometer (Shore-D DIN 53505, Hiroshima) was used to examine the hardness of Sr/Zn-doped CPP/GNS/UHMWPE composites samples. At room temperature and with a relative humidity of 30%, the specimens ($80 \times 10 \times 4$ mm^3) were placed on the platform of the testing instrument and the value of hardness was read thrice at three different spots which were a distance of 5 mm from each other. 10% (w/w) Sr–Zn-doped CPP/UHMWPE was set as a control.

Impact strength of Sr/Zn-doped CPP/GNS/UHMWPE

A drop weight impact tester (China) was used to measure the Charpy impact strength of Sr/Zn-doped CPP/GNS/UHMWPE composites samples. The bottoms of the samples with a 2 mm notch in the middle were fixed firmly into the groove of the instrument platform. After releasing the pendulum at a fixed height, the values of impact energy were respectively recorded. 10% (w/w) Zn/Sr/CPP/UHMWPE was also set as a control.

Tribology of Sr/Zn-doped CPP/GNS/UHMWPE

A friction and wear testing machine (UMT-3, BRUKER) was used to simulate the contact conditions in applications at a temperature of 37 °C and with a relative humidity of 30%. The wear tests of Sr/Zn-doped CPP/GNS/UHMWPE composite samples were carried out with a load of 100 N, and a sliding speed of 10 cm s^{-1} (600 rpm), and a sliding distance of 72 m (18 000 cycles). In the tribology tests, we chose a GCR15 stainless steel ball with a hardness value of RC 61 and a diameter of 10 mm as the counterpart. The coefficient of friction (COF), wear weight, and wear volume of various samples were recorded and analyzed. The micro-morphology of the worn surfaces of Sr/Zn-doped CPP/GNS/UHMWPE composite samples were observed with a 3D scanner. 10% (w/w) Sr/Zn-doped CPP/UHMWPE was set as a control.

Morphology of Sr/Zn-doped CPP/GNS/UHMWPE

A Scanning Electron Microscope (JSM-5900LV, JEOL) was used to characterize the micro-morphology of cross-sections of samples caused by liquid nitrogen brittle fracture. The observation was carried at a magnification of 4000× and an accelerating voltage of 20 kV. 10% (wt.) Sr/Zn-doped CPP/UHMWPE was set as a control.

Particles of Sr/Zn-doped CPP/GNS/UHMWPE composites and their effect on the proliferation of MC3T3-E1 cells

MC3T3-E1 cell lines (West China Hospital, Sichuan University) were cultured in MEM medium (Gibco) supplemented with 10% fetal calf serum (Gibco) and 1% penicillin/streptomycin (Hyclone) and incubated at 37 °C in a 5% CO_2 humidified atmosphere. Cells from passage 3 were used for challenging with various particles collected from the tribology tests. To investigate the effects of Sr/Zn-doped CPP/GNS/UHMWPE particles on the proliferation of MC3T3-E1 cells, the content of Sr/Zn-doped CPP/GNS in Sr/Zn-doped CPP/GNS/UHMWPE composites was set to 0%, 2%, 4%, 6%, 8% and 10%. Pure UHMWPE was set as a control. Due to the low specific gravity of UHMWPE, the agarose method was chosen to solve this problem. 6% (wt) agarose solution (GR, Life Technologies) was injected at high speed onto the bottom of 24 wells. Then the sample powders evenly adhered to the surface of the solidified agarose gels. All wells were sterilized using irradiation at 25 kGy (Sichuan Institute of Atomic Energy) for co-culture with MC3T3-E1 cell lines.

The P3 generation of MC3T3-E1 was seeded at a density of 1×10^4 cells per ml and incubated with 500 μL of complete medium in each well prepared at 37 °C in a 5% CO_2 humidified atmosphere. At predetermined time points (1, 3 and 5 days) ($n = 3$), the effect of particles on cell proliferation was measured using a cell counting kit-8 (CCK-8) assay according to the following method: 50 μL of CCK-8 (Biosharp) was added to each well; after reacting for 0.5 h in the incubator, the supernatant was transferred to a 96-well plate and measured at 450 nm with a micro-plate reader (MULTISKAN, FC, WALTHAM, MA, USA).

Calcein/PI Live/Dead viability/cytotoxicity assay

A Calcein/PI Live/Dead Viability/Cytotoxicity Assay Kit was used to study the cell viability of MC3T3-E1 cells in the extracts of Sr/Zn-doped CPP/GNS/UHMWPE samples.

Analysis of OPG/RANKL released from MC3T3-E1 cells by ELISA statistical analysis

Co-culturing between various particles of Sr/Zn-doped CPP/GNS/UHMWPE composites and MC3T3-E1 cells was carried out according to the agarose method. After two days of co-cultivation, the supernatant was collected and centrifuged for subsequent testing. The OPG and RANKL protein levels released from MC3T3-E1 were quantificationally measured using commercially available double ligand enzyme-linked immunosorbent ELISA reagents (Biosharp). The ELISA assay was carried out according to the manufacturer's instructions (R&D Corp). The concentrations of OPG and RANKL released from MC3T3-E1 cells were determined by standard curve and calculation.

Statistical analysis

SPSS (V26.0) was used to conduct the statistical analysis. Experimental data are presented as mean ± standard deviation

(SD). Results were analyzed by one-way ANOVA with Student's *t*-test. Statistical significance was set as $P < 0.05$.

Results and discussion

Characterization of Sr/Zn-doped CPP/GNS and Sr/Zn-doped CPP/GNS/UHMWPE

FTIR analysis. The FTIR analysis of the samples is shown in Fig. 1. Compared with the spectra of Sr-doped CPP, we could find no new characteristic peaks appearing in the spectra of Sr/Zn-doped CPP. As shown in Fig. 1a, significant chemical bands at 1284.97 cm^{-1}, 915.38 cm^{-1} and 779.84 cm^{-1} corresponded strongly to the stretching vibrations of "O–P═O" functional groups, "P–O–P" functional groups and "O–P–O" functional groups in Sr/Zn-doped CPP powders, respectively. These bands revealed polymerization at a hot temperature, which showed the successful preparation of Sr/Zn-doped CPP. It also indicated that the addition of a low dose of zinc had no effect on the FTIR spectra of Sr-doped CPP. As shown in Fig. 1b, the bands at 1238.69 cm^{-1} and 959.94 cm^{-1} were respectively attributed to the stretching vibrations of "O–P═O" and "P–O–P" functional groups in the mixing or sintering products of Sr/Zn-doped CPP and GNS, while the bands at 2291.54 cm^{-1} were attributed to carbon bonds from GNS. According to the results of the FTIR spectra, there were no new chemical bonds created in Sr/Zn-doped CPP/GNS during spark plasma sintering, which indicated that spark plasma sintering does not result in a chemical reaction.

XPS and EDS analysis. The X-ray photoelectron spectroscopy (XPS) measurements of Sr/Zn-doped CPP/GNS powders are shown in Fig. 2a–d.

The existence of Sr and Zn was recognized by the presence of the significant peaks of Sr 3d and Zn 2p in the XPS analysis. In addition, only GNS contained C. Thus, the presence of the C 1s peak in XPS analysis suggested the combination of Sr/Zn-doped CPP and graphene nanosheets (GNS). The existence of carbon, calcium, strontium, and zinc in Sr/Zn-doped CPP/GNS/UHMWPE was recognized by EDS analysis in Fig. 2e, which indicated the successful combination of Sr/Zn-doped CPP/GNS and UHMWPE by the hot press process.

Hardness of Sr/Zn-doped CPP/GNS/UHMWPE

The hardness of the Sr/Zn-doped CPP/GNS/UHMWPE composites is shown in Fig. 3a. The change in hardness depended on the content of reinforcement filler (Sr/Zn-doped CPP/GNS). The

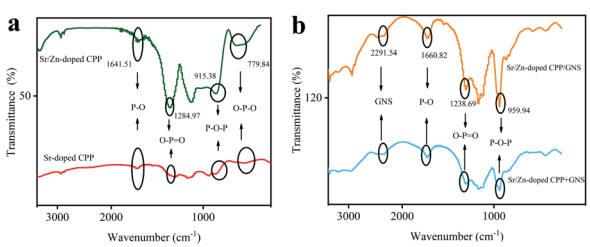

Fig. 1 FTIR patterns of various powders: (a) Sr/Zn-doped CPP and Sr-doped CPP; (b) Sr/Zn-doped CPP/GNS and Sr/Zn-doped CPP + GNS.

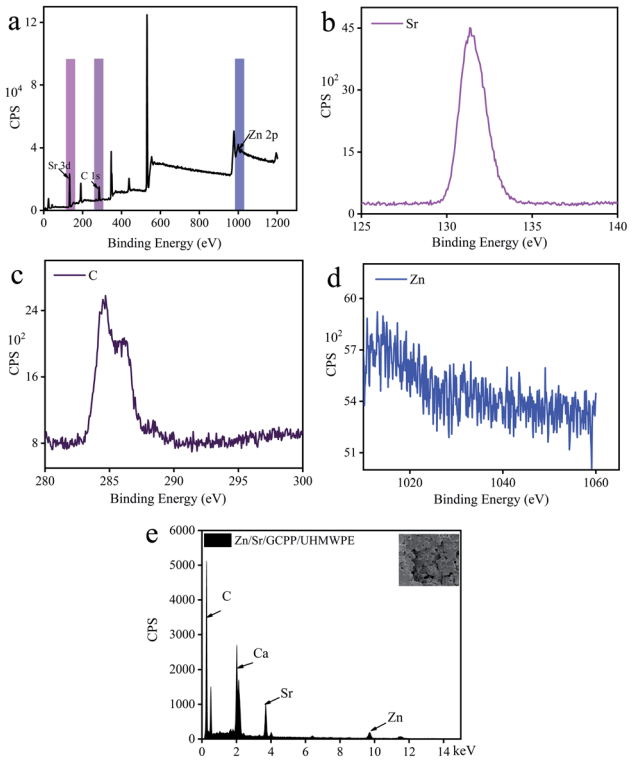

Fig. 2 XPS and EDS analysis of various specimens: (a–d) XPS of Sr/Zn-doped CPP/GNS; (e) EDS of Sr/Zn-doped CPP/GNS/UHMWPE.

average hardness of pure UHMEPE was 70.67 HA. For 5% Sr/Zn-doped CPP/GNS/UHMWPE composite materials, their average hardness was 86.43 HA. Meanwhile, the average hardness of 10% Sr/Zn-doped CPP/GNS/UHMWPE was as high as 89.83 HA. As the mass fraction of reinforcement filler (Sr/Zn-doped CPP/GNS) increased, the hardness of Sr/Zn-doped CPP/GNS/UHMWPE composites slowly increased: the average value of hardness went up to 91.67, 92.83, and 92.67 HA for composites of 15% Sr/Zn-doped CPP/GNS/UHMWPE, 20% Sr/Zn-doped CPP/GNS/UHMWPE and 30% Sr/Zn-doped CPP/GNS/UHMWPE, respectively. The average hardness of the composite materials was about 22% higher than that of pure UHMWPE. Thus, the hardness of the composite materials was affected by the content of reinforcement filler, and the addition

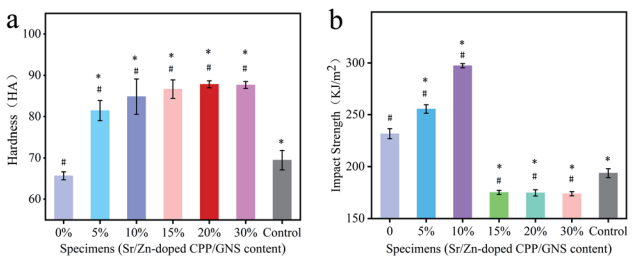

Fig. 3 Hardness and impact strength of Sr/Zn-doped CPP/GNS/UHMWPE composites with various Sr/Zn-doped CPP/GNS contents: (a) hardness; (b) impact strength ($n = 3$, * means the difference attained a statistically significant difference compared to the pure UHMWPE group, $p < 0.05$; # means the difference attained a statistically significant difference compared to the control group, $p < 0.05$).

of a suitable amount of reinforcement filler could improve the hardness. The reason for this phenomenon was that Sr/Zn-doped CPP/GNS had excellent mechanical properties, which could carry and transfer part of the load in the UHMWPE matrix.[20,21] The significant difference between the specimens and the control samples indicated that graphene nanosheets could improve the affinity between the filler and the matrix material, and then the hardness of the composites was enhanced by Sr/Zn-doped CPP/GNS.[22]

Impact strength of Sr/Zn-doped CPP/GNS/UHMWPE

The impact strength was calculated according to the following formula: $a_n = \frac{w_n}{h_n \times b_n} \times 10^3$. In this formula, the meaning of each symbol is as follows: a_n (kJ m^{-2}) represents the value of impact strength; w_n (kJ) represents the value of impact energy; h_n (mm) represents the height of specimen; b_n (mm) represents the remaining width of the notch at the bottom of the specimen.

Fig. 3b shows the impact strength of the Sr/Zn-doped CPP/GNS/UHMWPE composites. The impact strength of the composite materials was significantly influenced by the content of Sr/Zn-doped CPP/GNS fillers. The impact strength of pure UHMWPE was 231.67 kJ m^{-2}. After adding Sr/Zn-doped CPP/GNS, the average value of impact strength went up to 255.47 kJ m^{-2} and 297.29 kJ m^{-2} for 5% Sr/Zn-doped CPP/GNS/UHMWPE and 10% Sr/Zn-doped CPP/GNS/UHMWPE, respectively. Compared with pure UHMWPE, the average impact strengths of 5% Sr/Zn-doped CPP/GNS/UHMWPE and 10% Sr/Zn-doped CPP/GNS/UHMWPE in this study were about 10% higher. The increase in impact strength could be explained by the dispersion of fillers. In this situation, Sr/Zn-doped CPP/GNS fillers could disperse well and be closely combined with the UHMWPE matrix. To a certain extent, Sr/Zn-doped CPP/GNS fillers could disperse the stress and absorb the impact energy when composite materials were impacted by an external force.[21] Therefore, the impact strength of the composite material was improved. Meanwhile, the impact strengths of 5% Sr/Zn-doped CPP/GNS/UHMWPE and 10% Sr/Zn-doped CPP/GNS/UHMWPE were significantly better than Sr/Zn-doped CPP/UHMWPE (control) due to improved affinity between the filler and the matrix materials by the addition of GNS.[8]

However, excessive addition of fillers (Sr/Zn-doped CPP/GNS) severely weakened the impact strength of Sr/Zn-doped CPP/GNS/UHMWPE composites: the average values of the impact strength went down to 175.0 kJ m^{-2}, 174.58 kJ m^{-2} and 173.35 kJ m^{-2} for 15% Sr/Zn-doped CPP/GNS/UHMWPE, 20% Sr/Zn-doped CPP/GNS/UHMWPE and 30% Sr/Zn-doped CPP/GNS/UHMWPE, respectively. Excessive addition of fillers in the matrix hindered the combination between filler and matrix materials and resulted in the existence of voids and agglomerates, which reduced the ability of the composite materials to absorb stress and impact energy by forming weak points of stress concentration around the enhanced-particles.[23] In addition, the poor adhesion of fillers to the matrix materials caused by large agglomerates resulted in the fillers falling off the matrix under impact force, which significantly reduced the impact strength of the composite material.[24] Thereby, the impact strength of the composite material was reduced when the content of fillers exceeded the appropriate range.

Morphology observation of Sr/Zn-doped CPP/GNS/UHMWPE

10% Sr/Zn-doped CPP/GNS/UHMWPE was selected as the model for micro-structural analysis due to its good performance on hardness and impact strength. As presented in Fig. 4, we found that the incorporation of fillers into UHMWPE changed the micro-structure of UHMWPE, and fillers were well dispersed within the UHMWPE matrix and also closely combined with the UHMWPE matrix. In this way, part of the external load was carried and transferred by the fillers.[25,26] Thus, the hardness of composite materials was improved. As presented in Fig. 4a–c, the micro-structure of UHMWPE was dense and regular. Meanwhile, the cross-section micro-morphology of 10% Sr/Zn-doped CPP/GNS/UHMWPE composite material (Fig. 4g–i) was "cotton-like" with a regular size, which had the ability to disperse the stress and absorb external impact energy. Thus, the impact strength of this composite material was improved. Comparing the cross-section micro-morphology of 10% Sr/Zn-doped CPP/UHMWPE composite material (control) (Fig. 4d–f) with that of 10% Sr/Zn-doped CPP/GNS/UHMWPE composite material (Fig. 4g–i), we found that the addition of GNS into the fillers resulted in a "looser cotton-like" inner-structure. This structure increased the effective interface area between Sr/Zn-doped CPP/GNS fillers and the UHMWPE matrix, so this material was more effective for the initiation and termination of silver streaks when impacted.[27] In addition, the relative slippage occurring between fillers preceded the deformation of the polymer matrix.[28] Both behaviors above required the absorption of energy, which gave 10% Sr/Zn-doped CPP/UHMWPE

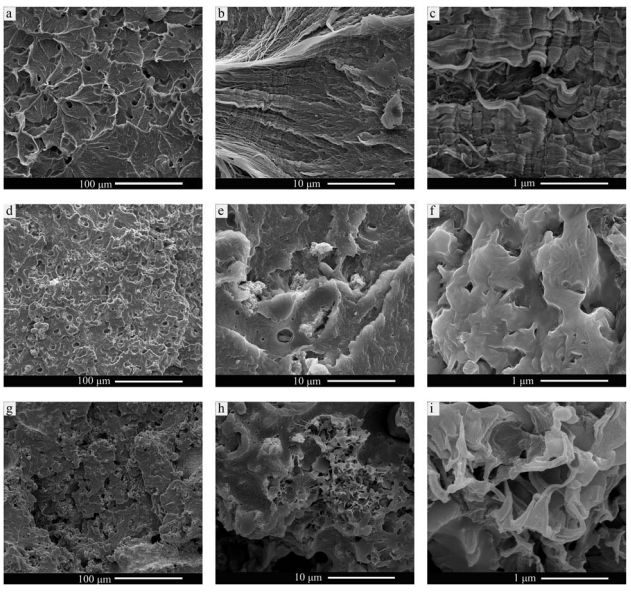

Fig. 4 The SEM images: (a–c) the cross-section of UHMWPE material; (d–f) the cross-section of 10% Sr/Zn-doped CPP/UHMWPE composite material; (g–i) the cross-section of 10% Sr/Zn-doped CPP/GNS/UHMWPE composite material.

composite material better ability to disperse the external force and absorb the impact energy.[21] In this way, the hardness and impact strength of the composite material were improved.

Tribology of Sr/Zn-doped CPP/GNS/UHMWPE

Analysis of wear particles mass volume and coefficient of friction (COF). Fig. 5a shows the analysis of the wear particle weights of various samples. Compared with the pure UHMWPE group, the weight values of wear particles of 5% Sr/Zn-doped CPP/GNS/UHMWPE and 10% Sr/Zn-doped CPP/GNS/UHMWPE composites were lower. Among them, 5% Sr/Zn-doped CPP/GNS/UHMWPE composite materials showed the lowest value. On the one hand, the Sr/Zn-doped CPP/GNS particles that were uniformly dispersed in the UHMWPE matrix could preferentially support part of the load as fulcrums.[29] In the friction process, the Sr/Zn-doped CPP/GNS particles can effectively disperse, transfer and support the carried load and shear force, which limited the movement of UHMWPE molecules.[30] On the other hand, the filling of Sr/Zn-doped CPP/GNS particles also improved the strength of the composite materials and played a role in the enhancement, so UHMWPE molecules could not easily escape from the matrix.[31] Thereby, the wear resistance of the composite material was greatly improved. Meanwhile, the superiority in wear particle weight for these two Sr/Zn-doped CPP/GNS/UHMWPE composites compared to the control sample indicated that the addition of graphene nanosheets could promote inter-facial compatibility between fillers and matrix, which could improve the wear performance of composite materials.

The wear particle weight increased as the content of Sr/Zn-doped CPP/GNS added into the UHMWPE matrix increased. When the content of Sr/Zn-doped CPP/GNS fillers reached 20%, the weight value of the wear particles was higher than that of pure UHMWPE and its wear resistance showed a deterioration. This could be attributed to the uneven distribution of these inorganic particle-fillers in the matrix.[32] The agglomeration phenomenon caused by excessive addition resulted in the blocking of the UHMWPE molecular chain.[32,33] Thereby, the wear resistance of composite material was weakened.

The analysis of wear volume and coefficient of friction (COF) are shown in Fig. 5b and c, and their change trends were inconsistent with that of wear weight. 10% Sr/Zn-doped CPP/GNS/UHMWPE composite material showed the lowest value in wear COF.

Fig. 5d shows an analysis of the real-time friction coefficient. At the beginning of friction, the wear COFs of various samples were low. The main reason for this phenomenon was that the initial contacts between samples and counterparts were established on their rough and hard surfaces.[34,35] During the friction process, the COF gradually increased to a certain value and was maintained. This phenomenon was due to the fact that the area of the contact surface became larger with the friction process. Therefore, the COF remained stable when the area of the contact surface was constant. Compared with the pure UHMWPE sample, 5% Sr/Zn-doped CPP/GNS/UHMWPE and 10% Sr/Zn-doped CPP/GNS/UHMWPE composites presented a lower initial COF and reached steady states of COF earlier, which corresponded to their lower values of wear weight and wear volume.

Compared with the pure UHMWPE sample, the initial COFs of 15% Sr/Zn-doped CPP/GNS/UHMWPE, 20% Sr/Zn-doped CPP/GNS/UHMWPE and 30% Sr/Zn-doped CPP/GNS/UHMWPE composites were higher. Thus, the appropriate addition of fillers into the UHMWPE matrix could enhance the wear performance of composites. However, excessive addition of fillers into the UHMWPE matrix resulted in an uneven surface, grooves, and cracks, which were likely to result in poor friction performance.[36] Compared with the control sample (10% Sr/Zn-doped CPP/UHMWPE), 10% Sr/Zn-doped CPP/GNS/UHMWPE presented much better wear resistance, indicating that the addition of GNS was conducive to the improvement in affinity between fillers and matrix materials.[37]

Morphology of Sr/Zn/G-CPP/UHMWPE processed by friction. Fig. 6 shows the effects of different contents of Sr/Zn-doped CPP/GNS fillers on the friction morphology of Sr/Zn-doped CPP/GNS/UHMWPE composites. Fig. 6a–d show the regular grooves and Fig. 6e and f show an uneven friction surface. The wear mechanism of the composite materials was complicated. Generally, it existed in a mixed form. In the wear process, the transfer film was formed on the surface of the counter-face ball, which enhanced the wear performance and formed a relatively flat surface. Therefore, the wear mechanism of UHMWPE is mainly adhesion wear.[38]

At the same time, the depth values of the grooves were also observed. Compared with pure UHMWPE, we found that the addition of Sr/Zn-doped CPP/GNS fillers into the UHMWPE matrix reduced the groove depth, which meant an improvement in wear performance. However, the depth values of the grooves for 15% Sr/Zn-doped CPP/GNS/UHMWPE and 20% Sr/Zn-doped

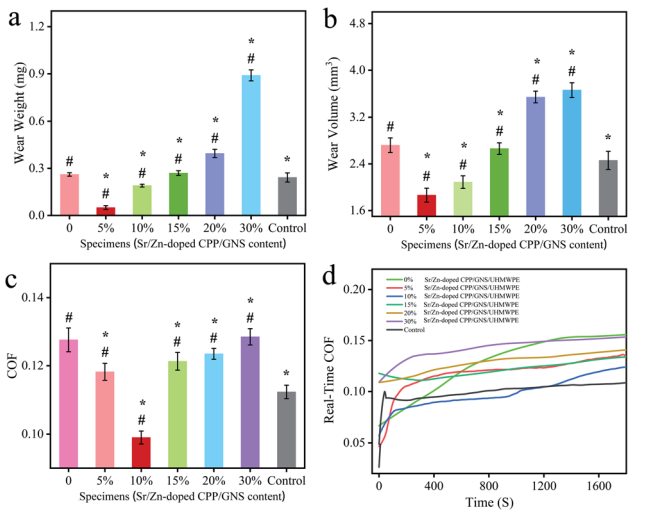

Fig. 5 Wear behavior of Sr/Zn-doped CPP/GNS/UHMWPE composite with various Sr/Zn-doped CPP/GNS contents: (a) wear weight; (b) wear volume; (c) wear COF; (d) real-time wear COF ($n = 3$, * means the difference attained a statistically significant difference compared to the pure UHMWPE group, $p < 0.05$; # means the difference attained a statistically significant difference compared to the control group, $p < 0.05$).

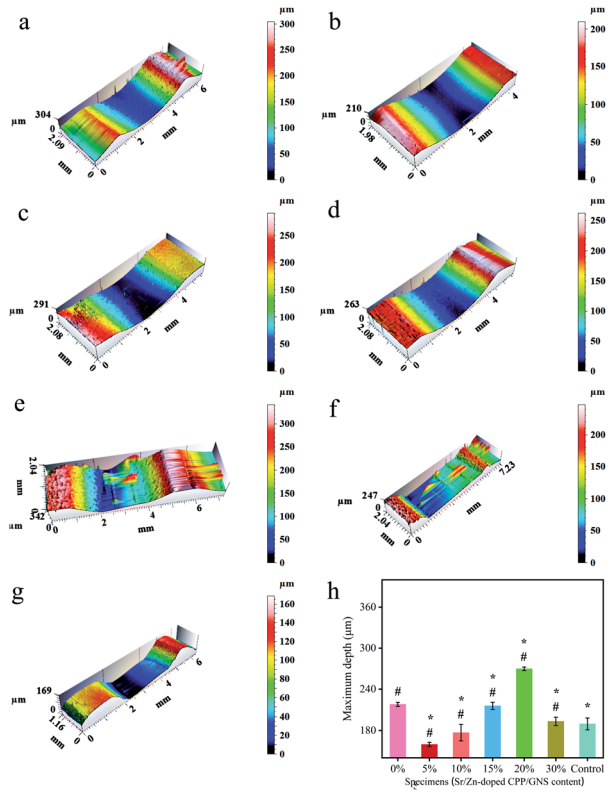

Fig. 6 The morphology of various samples: (a) pure UHMWPE; (b) 5% Sr/Zn-doped CPP/GNS/UHMWPE; (c) 10% Sr/Zn-doped CPP/GNS/UHMWPE; (d) 15% Sr/Zn-doped CPP/GNS/UHMWPE; (e) 20% Sr/Zn-doped CPP/GNS/UHMWPE; (f) 30% Sr/Zn-doped CPP/GNS/UHMWPE; (g) control; (h) the maximum depth of various samples ($n = 5$, * means the difference attained a statistically significant difference compared to pure UHMWPE group, $p < 0.05$; # means the difference attained a statistically significant difference compared to control group, $p < 0.05$).

CPP/GNS/UHMWPE increased with an increase in filler content. The depth value of the grooves for 30% Sr/Zn-doped CPP/GNS/UHMWPE composite was lower than for pure UHMWPE. Meanwhile, the bottoms of these grooves were longer. The main reason for this phenomenon was that the Sr/Zn/GCPP fillers added in excess into UHMWPE could not be well integrated into the UHMWPE matrix and changes in internal structures directly affected wear performance.[36]

Cell proliferation and OPG and RANKL secretion from MC3T3-E1 cells being challenged by wear particles

The effect of particles on the proliferation of MC3T3-E1 cells. An *in vitro* study revealed the positive effects of wear particles on the growth and proliferation of MC3T3-E1 cell lines, which changed the expression of various molecular factors from the 1st to the 5th day.[39] Therefore, we researched the effect of wear particles of various samples on MC3T3-E1 on the 1st, 3rd and 5th days by the CCK-8 method. Fig. 7a shows the growth result of MC3T3-E1 challenged by various wear particles of composite materials. No significant cytotoxicity was observed for any sample. The relative growth rate (the ratio of the OD value of the sample to the OD value of the blank control sample, RGR) showed that cell proliferation increased during the co-culture process. RGR revealed that cell proliferation increased with the prolonging of culture time in each group. Moreover, the RGR of MC3T3-E1 challenged by various wear particles of composite materials increased in an Sr/Zn-doped CPP/GNS content-dependent way during the entire co-culture period. In this study, the proliferation rate of MC3T3-E1 challenged by wear particles of Sr/Zn-doped CPP/GNS/UHMWPE composites was significantly higher than that of cells challenged by SCPP/UHMWPE wear particles obtained in our previous study. The wear particles obtained from 6%, 8%, 10%, and 100% Sr/Zn-doped CPP/GNS/UHMWPE composites could even promote cell growth. We deduced that Sr and Zn have a synergistic effect in promoting the proliferation of MC3T3-E1 cells. In order to prove this inference, the effectiveness value of ions was calculated according to the following formula:

$$E_i = \frac{RGR_i - RGR_{CPP}}{RGR_{CPP}} \times 100\%$$

In this formula, the meaning of each symbol is as follows: E_i represents the effectiveness value of different samples; RGR_i represents the relative growth factor of different samples. The analysis is shown in Fig. 7b. The effectiveness value of 8% Sr/0.25% Zn-doped CPP was higher than the sum of 0.25% Zn-doped CPP and 8% Sr-doped CPP. Thus, we deduced that Sr and Zn have a synergistic effect in promoting the proliferation of MC3T3-E1 cells after introducing Sr and Zn into CPP.

The bio-property of Sr/Zn-doped CPP/GNS/UHMWPE wear particles had a significant influence on resisting aseptic loosening. The aseptic loosening of artificial joints is caused by periprosthetic osteolysis resulting from the harmful effects (destroying the growth of osteoblasts) on osteoblasts exerted by UHMWPE particles around prostheses.[25,40] The addition of Sr/Zn-doped CPP/GNS could alleviate these harmful effects due to its great promotion effect on the proliferation of osteoblasts, and then be beneficial to the formation of bone and resisting aseptic loosening.

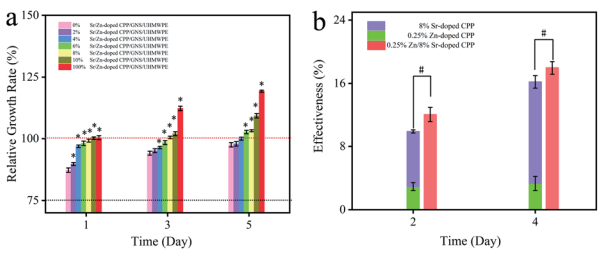

Fig. 7 The relative growths rate of various samples: (a) 0% Sr/Zn-doped CPP/GNS/UHMWPE, 2% Sr/Zn-doped CPP/GNS/UHMWPE, 4% Sr/Zn-doped CPP/GNS/UHMWPE, 6% Sr/Zn-doped CPP/GNS/UHMWPE, 8% Sr/Zn-doped CPP/GNS/UHMWPE, 10% Sr/Zn-doped CPP/GNS/UHMWPE and 100% Sr/Zn-doped CPP/GNS/UHMWPE; (b) 8% Sr-doped CPP, 0.25% Zn-doped CPP and 0.25%Zn/8% Sr-doped CPP. ($n = 3$, * means the difference attained a statistically significant difference compared to the pure UHMWPE group, $p < 0.05$; # means the difference attained a statistically significant difference compared to 0.25% Zn-8% Sr-doped CPP group, $p < 0.05$).

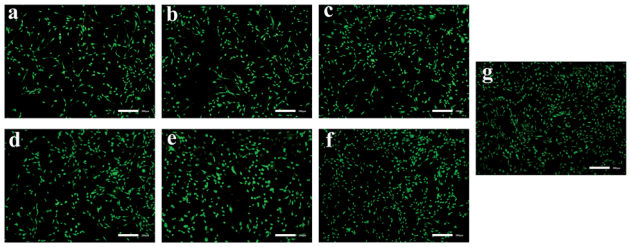

Fig. 8 The morphology of various samples: (a) 0% Sr/Zn-doped CPP/GNS/UHMWPE; (b) 5% Sr/Zn-doped CPP/GNS/UHMWPE; (c) 10% Sr/Zn-doped CPP/GNS/UHMWPE; (d) 15% Sr/Zn-doped CPP/GNS/UHMWPE; (e) 20% Sr/Zn-doped CPP/GNS/UHMWPE; (f) 30% Sr/Zn-doped CPP/GNS/UHMWPE; (g) 100% Sr/Zn-doped CPP/GNS/UHMWPE.

Calcein/PI Live/Dead viability/cytotoxicity assay. As shown in Fig. 8, the viability of MC3T3-E1 cells in the extracts of various samples increased in an Sr/Zn-doped CPP/GNS content-dependent way. The number of live cells in the extracts of 100% Sr/Zn-doped CPP/GNS/UHMWPE was the highest, while the number of live cells in the extracts of 0% Sr/Zn-doped CPP/GNS/UHMWPE was the lowest. In short, the addition of Sr/Zn-doped CPP/GNS into UHMWPE could promote cell proliferation and cell viability.

The effect of particles on OPG and RANKL secretion from MC3T3-E1 cells. OPG (osteoprotegerin) and RANKL (receptor activator of nuclear factor-κ B ligand) are important regulators in the process of osteogenesis around the prosthesis. Considered as a decoy receptor of RANKL, OPG can inhibit proliferation and differentiation of osteoclasts by combining with RANKL.[41] Maintaining the balance between OPG and RANKL can regulate the formation of osteoclasts in periprosthetic tissues. Thus, the secretion of OPG and RANKL, and the ratio of OPG and RANKL from MC3T3-E1 cells at 48 h were investigated in this study.

From Fig. 9, we can observe that the secretion of OPG from MC3T3-E1 cells in each group increased with an increase in Sr/Zn-doped CPP/GNS content after 48 h. However, the secretion of RANKL by MC3T3-C1 cells in each group fell with the increase in Sr/Zn-doped CPP/GNS content. In this way, the ratio of OPG to RANKL rose with an increase in Zn/Sr/GCPP content. Among all test groups, the Sr/Zn-doped CPP/GNS group illustrated the highest ratio and the UHMWPE group showed the lowest ratio. Our study (ESI†) has proved that the Sr/Zn-doped CPP/GNS particles could increase the OPG/RANKL ratio, and the OPG/RANKL ratio presented from MC3T3-E1 challenged by Sr/Zn-doped CPP/GNS particles was significantly higher than that of cells challenged by Sr-doped CPP particles. This might be due to the Sr/Zn-doped CPP/GNS particles exerting their stronger therapeutic effect by down-regulating sclerostin, thereby activating the Wnt/beta-catenin signal pathway.[42] Considering all the above factors, the addition of Sr/Zn-doped CPP/GNS particles into UHMWPE could perform on osteoblast cells to alter the OPG/RANKL ratios and greatly promote the proliferation of osteoblasts; as a result, osteoclastogenesis was inhibited. Therefore, the addition of Sr/Zn-doped CPP/GNS fillers into UHMWPE could enhance the ability of Sr/Zn-doped CPP/GNS/UHMWPE composites to resist aseptic loosening.

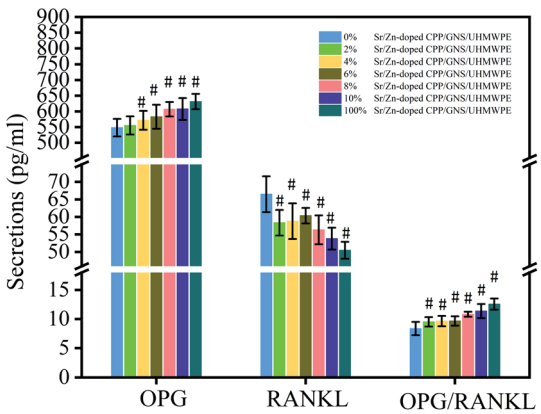

Fig. 9 The effect of various wear particles on OPG, RANKL, and OPG/RANKL ratio from MC3T3-E1 at 48 h ($n = 3$, # means the difference attained a statistically significant difference compared to 0% Zn/Sr/GCPP/UHMWPE group, $p < 0.05$).

Conclusions

The aseptic loosening of an artificial joint resulting from the wear particles of artificial joint components could shorten the service life of the artificial joint and bring great pain to patients. In this study, we synthesized a new class of metalo-organic particle-fillers (Sr/Zn-doped CPP/GNS) to enhance UHMWPE. The Sr/Zn-doped CPP/GNS/UHMWPE composites showed good comprehensive performances in terms of hardness, impact strength, and tribology. Moreover, Sr/Zn-doped CPP/GNS/UHMWPE composites could promote the secretion of OPG from osteoblasts and inhibit the secretion of RANKL from osteoblasts, thus increasing the OPG/RANKL ratio. In general, 10% Sr/Zn-doped CPP/GNS/UHMWPE showed an optimal effect in physicochemical properties and bio-properties above all other samples. Therefore, the composites had the potential efficacy to prevent and treat aseptic loosening. In summary, Sr/Zn-doped CPP/GNS/UHMWPE composites with a suitable Sr/Zn-doped CPP/GNS content would be a useful material for fabricating artificial joint components with the ability to resist aseptic loosening for its excellent comprehensive performance.

Conflicts of interest

There are no conflicts to declare.

Acknowledgements

The authors would like to thank the Key Research and Development Program of Sichuan Province (2019YFS0121).

Notes and references

1 S. K. Mamidi, K. Klutcharch, S. Rao, J. C. M. Souza, L. G. Mercuri and M. T. Mathew, *Biomed. Eng. Lett.*, 2019, **9**, 169–179.

2 N. A. Patil, J. Njuguna and B. Kandasubramanian, *Eur. Polym. J.*, 2020, **125**, 22.
3 J. Pajarinen, T. H. Lin, T. Sato, Z. Yao and S. B. Goodman, *J. Mater. Chem. B*, 2014, **2**, 7094–7108.
4 J. C. Baena, J. P. Wu and Z. X. Peng, *Lubricants*, 2015, **3**, 413–436.
5 A. Wang, H. Zeng, S. S. Yau, A. Essner, M. Manely and J. Dumbleton, *J. Phys. D: Appl. Phys.*, 2006, **39**, 3213–3219.
6 A. M. Kandahari, X. L. Yang, K. A. Laroche, A. S. Dighe, D. F. Pan and Q. J. Cui, *Bone Res.*, 2016, **4**, 13.
7 Y. Abu-Amer, I. Darwech and J. C. Clohisy, *Arthritis Res. Ther.*, 2007, **9**, 7.
8 A. Sobajima, T. Okihara, S. Moriyama, N. Nishimura, T. Osawa, K. Miyamae, H. Haniu, K. Aoki, M. Tanaka, Y. Usui, K.-i. Sako, H. Kato and N. Saito, *ACS Biomater. Sci. Eng.*, 2020, **6**, 7032–7040.
9 F. Mindivan and A. Colak, *J. Appl. Polym. Sci.*, 2021, **138**, 13.
10 X. H. Chen, S. Zhang, L. Zhang, P. Zhu and G. Q. Zhang, *Polymers*, 2021, **13**, 14.
11 Z. P. Gu, B. X. Huang, Y. W. Li, M. Tian, L. Li and X. X. Yu, *Mater. Sci. Eng., C*, 2016, **61**, 526–533.
12 Z. Cu, X. Zhang, L. Li, Q. Wang, X. Yu and T. Feng, *Mater. Sci. Eng., C*, 2013, **33**, 274–281.
13 C. C. Huang, L. Li, X. X. Yu, Z. P. Gu and X. Zhang, *Biomed. Mater.*, 2014, **9**, 10.
14 Z. P. Gu, H. Wang, L. Li, Q. G. Wang and X. X. Yu, *Biomed. Mater.*, 2012, **7**, 9.
15 R. Cruz, J. Calasans-Maia, S. Sartoretto, V. Moraschini, A. M. Rossi, R. S. Louro, J. M. Granjeiro and M. D. Calasans-Maia, *Ceram. Int.*, 2018, **44**, 1240–1249.
16 A. M. Shafeek, M. H. Khedr, S. I. El-Dek and N. Shehata, *Appl. Nanosci.*, 2020, **10**, 3603–3615.
17 G. A. Fielding, N. Sarkar, S. Vahabzadeh and S. Bose, *J. Funct. Biomater.*, 2019, **10**, 13.
18 Y. H. Han, R. Q. Gao, I. Bajpai, B. N. Kim, H. Yoshida, A. Nieto, H. W. Son, J. Yun, B. K. Jang, S. Jhung, J. M. Zhao, K. H. Hwang, F. Chen, J. F. Shackelford and S. Kim, *Adv. Appl. Ceram.*, 2020, **119**, 57–74.
19 Z.-H. Zhang, Z.-F. Liu, J.-F. Lu, X.-B. Shen, F.-C. Wang and Y.-D. Wang, *Scr. Mater.*, 2014, **81**, 56–59.
20 M. J. Martinez-Morlanes, F. J. Pascual, G. Guerin and J. A. Puertolas, *J. Mech. Behav. Biomed. Mater.*, 2020, **115**, 104248.
21 M. Padhan, A. Gulhane and J. Bijwe, *Surf. Topogr.: Metrol. Prop.*, 2020, **8**, 17.
22 H. S. Vadivel, A. Golchin and N. Emami, *Tribol. Int*, 2018, **124**, 169–177.
23 A. A. W. Anwer, T. Dong and H. E. Naguib, *Compos. Sci. Technol.*, 2020, **192**, 8.
24 S. V. Panin, Q. T. Huang, V. O. Alexenko, D. G. Buslovich, L. A. Kornienko, F. Berto, S. A. Bochkareva, I. L. Panov and N. V. Ryabova, *Appl. Sci.*, 2020, **10**, 30.
25 L. Xu, Y. Zheng, Z. Yan, W. Zhang, J. Shi, F. Zhou, X. Zhang, J. Wang, J. Zhang and B. Liu, *Appl. Surf. Sci.*, 2016, **370**, 201–208.
26 S. Wang, Q. Feng, J. Sun, F. Gao, W. Fan, Z. Zhang, X. Li and X. Jiang, *ACS Nano*, 2016, **10**, 298–306.
27 S. D. Han, T. C. Zhang, Y. H. Guo, C. H. Li, H. Wu and S. Y. Guo, *Polymer*, 2019, **182**, 11.
28 B. Y. Wu, Y. D. Cai, X. W. Zhao and L. Ye, *Polym. Test.*, 2021, **93**, 10.
29 M. J. Martinez-Morlanes, P. Castell, P. J. Alonso, M. T. Martinez and J. A. Puertolas, *Carbon*, 2012, **50**, 2442–2452.
30 A. V. Maksimkin, S. D. Kaloshkin, M. S. Kaloshkina, M. V. Gorshenkov, V. V. Tcherdyntsev, K. S. Ergin and I. V. Shchetinin, *J. Alloys Compd.*, 2012, **536**, S538–S540.
31 S. Gurgen, A. Sert and M. C. Kushan, *J. Appl. Polym. Sci.*, 2021, **138**, 13.
32 D. S. Xiong and Z. M. Jin, *Surf. Coat. Technol.*, 2004, **182**, 149–155.
33 S. R. Ge, Q. L. Wang, D. K. Zhang, H. Zhu, D. S. Xiong, C. H. Huang and X. L. Huang, *Wear*, 2003, **255**, 1069–1075.
34 J. L. Montes-Seguedo, I. Dominguez-Lopez and J. D. O. Barceinas-Sanchez, *Mater. Lett.*, 2021, **284**, 4.
35 X. Xie, Z. Guo and C. Yuan, *Polym. Compos.*, 2020, **41**, 5269–5280.
36 J. A. Puertolas and S. M. Kurtz, *J. Mech. Behav. Biomed. Mater.*, 2014, **39**, 129–145.
37 W. Zexiong, L. Anqi, Z. Zishou and M. Kancheng, *J. Therm. Anal. Calorim.*, 2020, DOI: 10.1007/s10973-020-10151-w.
38 Y. S. Kumar, K. V. S. R. Rao and Y. R. Sunil, *Int. J. Eng.*, 2020, **33**, 1560–1566.
39 R. Chiu, T. Ma, R. L. Smith and S. B. Goodman, *J. Biomed. Mater. Res., Part A*, 2009, **89**, 242–247.
40 S. W. Wang, Q. Feng, J. S. Sun, F. Gao, W. Fan, Z. Zhang, X. H. Li and X. Y. Jiang, *ACS Nano*, 2016, **10**, 298–306.
41 A. M. Kandahari, X. L. Yang, K. A. Laroche, A. S. Dighe, D. Pan and Q. J. Cui, *Bone Res.*, 2016, **4**, 13.
42 B. L. Wang, H. H. Guo, T. X. Geng, K. N. Sun, L. Zhang, Z. D. Lu and Q. H. Jin, *Biosci. Rep.*, 2021, **41**, 18.